AD-A158 852 FRACTOGRAPHY OF MIXED MODE I - II FAILURE IN GRAPHITE/EPOXY AND GRAPHITE/.. (U) AIR FORCE WRIGHT AERONAUTICAL LABS WRIGHT-PATTERSON AFB OH

1/1

UNCLASSIFIED S L DONALDSON JUN 85 AFWAL-TR-84-4186 F/G 11/4 NL

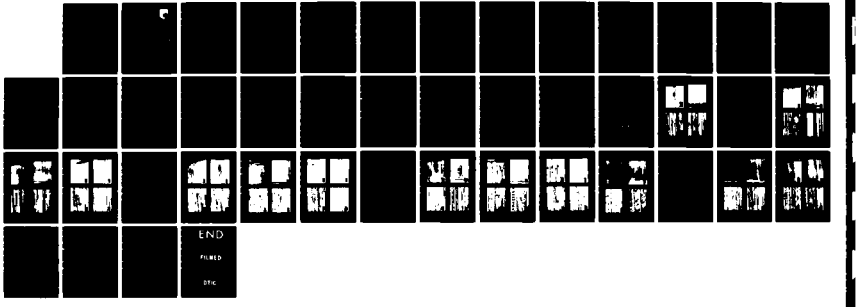

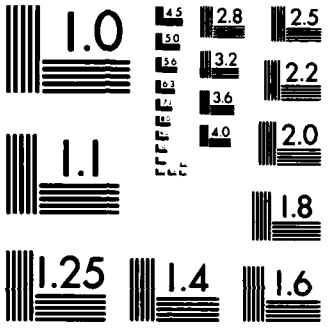


MICROCOPY RESOLUTION TEST CHART

(2)

AFWAL-TR-84-4186


# FRACTOGRAPHY OF MIXED MODE I - II FAILURE IN GRAPHITE/EPOXY AND GRAPHITE/THERMOPLASTIC UNIDIRECTIONAL COMPOSITES

Steven L. Donaldson

Mechanics & Surface Interactions Br
Nonmetallic Materials Division



June 1985





Approved for public release; distribution unlimited.

MATERIALS LABORATORY
AIR FORCE WRIGHT AERONAUTICAL LABORATORIES
AIR FORCE SYSTEMS COMMAND
WRIGHT-PATTERSON AIR FORCE BASE, OHIO 45433

*NOTICE*

*When Government drawings, specifications, or other data are used for any purpose other than in connection with a definitely related Government procurement operation, the United States Government thereby incurs no responsibility nor any obligation whatsoever; and the fact that the government may have formulated, furnished, or in any way supplied the said drawings, specifications, or other data, is not to be regarded by implication or otherwise as in any manner licensing the holder or any other person or corporation, or conveying any rights or permission to manufacture, use, or sell any patented invention that may in any way be related thereto.*

*This technical report has been reviewed and is approved for publication.*

Steven L. Donaldson

STEVEN L. DONALDSON
Materials Research Engineer
Mechanics & Surface Interactions Br

S.W. Tsai

STEPHEN W. TSAI, Chief
Mechanics & Surface Interactions Br
Nonmetallic Materials Division

*FOR THE COMMANDER:*

George E. Husman

GEORGE E. HUSMAN, Chief
Nonmetallic Materials Division

*"If your address has changed, if you wish to be removed from our mailing list, or if the addressee is no longer employed by your organization please notify* AFWAL/MLBM *,W-P AFB, OH 45433 to help us maintain a current mailing list".*

*Copies of this report should not be returned unless return is required by security considerations, contractual obligations, or notice on a specific document.*

SECURITY CLASSIFICATION OF THIS PAGE

# REPORT DOCUMENTATION PAGE

| | |
|---|---|
| 1a. REPORT SECURITY CLASSIFICATION: Unclassified | 1b. RESTRICTIVE MARKINGS |
| 2a. SECURITY CLASSIFICATION AUTHORITY | 3. DISTRIBUTION/AVAILABILITY OF REPORT: Approved for public release; distribution unlimited. |
| 2b. DECLASSIFICATION/DOWNGRADING SCHEDULE | |
| 4. PERFORMING ORGANIZATION REPORT NUMBER(S): AFWAL-TR-84-4186 | 5. MONITORING ORGANIZATION REPORT NUMBER(S) |
| 6a. NAME OF PERFORMING ORGANIZATION: Materials Laboratory; 6b. OFFICE SYMBOL (If applicable): AFWAL/MLBM | 7a. NAME OF MONITORING ORGANIZATION |
| 6c. ADDRESS (City, State and ZIP Code): Air Force Wright Aeronautical Laboratory, Wright Patterson AFB OH 45433 | 7b. ADDRESS (City, State and ZIP Code) |
| 8a. NAME OF FUNDING/SPONSORING ORGANIZATION; 8b. OFFICE SYMBOL (If applicable) | 9. PROCUREMENT INSTRUMENT IDENTIFICATION NUMBER |
| 8c. ADDRESS (City, State and ZIP Code) | 10. SOURCE OF FUNDING NOS. |

| PROGRAM ELEMENT NO. | PROJECT NO. | TASK NO. | WORK UNIT NO. |
|---|---|---|---|
| 61102F | 2307 | P2 | 01 |

11. TITLE (Include Security Classification): Fractography of Mixed Mode I-II Failure in Graphite/Epoxy & Graphite/Thermoplastic Unidirectional Composites

12. PERSONAL AUTHOR(S): Steven L. Donaldson

| 13a. TYPE OF REPORT | 13b. TIME COVERED | 14. DATE OF REPORT (Yr., Mo., Day) | 15. PAGE COUNT |
|---|---|---|---|
| Final Technical Report | FROM Feb TO Aug 84 | June 1985 | 44 |

16. SUPPLEMENTARY NOTATION: Sections of this report published in Composites, Vol 16, No. 2, pps 103-112, April 1985.

| 17. COSATI CODES | | |
|---|---|---|
| FIELD | GROUP | SUB. GR. |
| | | |
| | | |

18. SUBJECT TERMS (Continue on reverse if necessary and identify by block number): Composite materials, fracture, mixed-mode, Mode II, fractography, epoxy, thermoplastic, PEEK


19. ABSTRACT (Continue on reverse if necessary and identify by block number)

The notched off-axis tensile test and the notched three rail shear test were used to produce states of in-plane loading varying from pure Mode I (crack opening) to Mode II (forward shearing). The two material systems tested were Fiberite T300/1034C graphite/epoxy and Imperial Chemical Industries graphite reinforced polyetheretherketone thermoplastic composite (APC-1 PEEK).

Using a scanning electron microscope, a detailed examination of the resulting fracture surfaces was conducted. Results at magnification levels of 100X and 800X are presented. Very distinct changes can be observed in each material as the load ratio changes. In addition, for a fixed mixed mode load ratio, large differences can be seen in the matrix deformation patterns between the two material systems. Of particular interest are ductile spike formations seen in the highly shear loaded PEEK specimens. These observations provide some insight as to the increased toughness seen at higher Mode II ratios, and the increased toughness seen in the thermoplastic system.


| 20. DISTRIBUTION/AVAILABILITY OF ABSTRACT | 21. ABSTRACT SECURITY CLASSIFICATION |
|---|---|
| UNCLASSIFIED/UNLIMITED [X] SAME AS RPT [ ] DTIC USERS [ ] | Unclassified |

| 22a. NAME OF RESPONSIBLE INDIVIDUAL | 22b. TELEPHONE NUMBER (Include Area Code) | 22c. OFFICE SYMBOL |
|---|---|---|
| S. L. Donaldson | (513) 255-8206 | AFWAL/MLBM |

DD FORM 1473, 83 APR — EDITION OF 1 JAN 73 IS OBSOLETE.

SECURITY CLASSIFICATION OF THIS PAGE

FOREWORD

This report was prepared in the Mechanics and Surface Interactions Branch (AFWAL/MLBM), Nonmetallic Materials Division, Materials Laboratory, Air Force Wright Aeronautical Laboratories, Wright-Patterson Air Force Base, Ohio. The work was performed under the support of Project Number 2419, "Nonmetallic Structural Materials", Task Number 241903, "Composite Materials and Mechanics Technology."

The fractography was conducted while the author was a visiting researcher at the Linköping University Institute of Technology, Linköping, Sweden. A JEOL JSM- 15 Scanning electron microscope there was used for this study.

Sections of this report are to appear in the journal Composites.

TABLE OF CONTENTS

LIST OF FIGURES

# SECTION I

# INTRODUCTION

The past several years have shown an increase in understanding the factors involved in composite damage before final failure [1, 2]. Damage growth in composites falls into several main categories. The first of these is the development of intralaminar transverse cracks. Delamination, another form, is the development of cracks running in planes parallel to and between the lamina. Fatigue loading, transverse impact loading, and free edge stresses are several sources of these types of damage. Both types involve mostly matrix fracture, little fiber breakage occurs. The problem is aggravated by the brittle nature of current epoxy systems. Full exploitation of the high fiber stiffness and strength is often not obtained due to fracture mechanics considerations of the ply cracking and delamination phenomena.

The ability of a material to resist crack growth is its fracture toughness. Methods of characterizing fracture toughness in composites, as well as the search for tougher composite materials, is therefore an important issue.

In this study, transverse ply cracking under combined Mode I (crack opening) and Mode II (forward shearing) will be examined using the off-axis tension and notched three rail shear test. Although delamination occurs on planes orthogonal to the matrix cracking plane, the ply transverse cracking toughness can also yield some insight into a material's delamination toughness [3].

The fracture surfaces from graphite/epoxy (T300/1034C) and graphite/-thermoplastic (APC-1) composites will be compared. Gross deformation, at

100X, and detailed deformation, at 800X, will be examined to determine matrix deformation and fiber breakage patterns.

## SECTION II

## FABRICATION AND TESTING

Eight ply unidirectional panels of Fiberite T300/1034C were layed-up and cured following the manufacturer's recommendations. The panels were not post-cured. Eight ply unidirectional APC-1 PEEK panels were supplied already fabricated by Imperial Chemical Industries. Care was taken in specimen design that no fibers ran from one grip area to the opposite grip. Three specimens of each material at each orientation were tested.

In-plane cracks were formed by drilling a 0.381 mm (0.015 in) diameter pilot hole in the center of the specimen. A 0.127 mm (0.005 in) diameter diamond impregnated wire was fed through the hole, then used to extend the crack length to a total length of, typically, 5.08 mm (0.2 in). The cracks were cut parallel to the fibers. Typewriter correction fluid was applied to the crack tips before sharpening. Crack tips were then sharpened using a scalpel. After sharpening, magnification showed that a natural crack did extend slightly beyond the actual razor notch. The final specimen configuration is shown in Figure 1.

Specimens were tested at a crosshead speed of 0.762 mm/min (0.03 in/min). No rate effect was studied. Stress-strain responses were linear until unstable crack growth occurred. The cracks always ran from the crack tip, parallel to the fibers and the saw cut. The only deviation from this failure pattern were the PEEK compression specimens. In these specimens, loading was linear until a point at which the material, by plastic deformation, closed-up the gap made by the saw cut. The load dropped about 9% during this deformation. The unnotched specimen areas lying in the region between the end of the saw cut and the

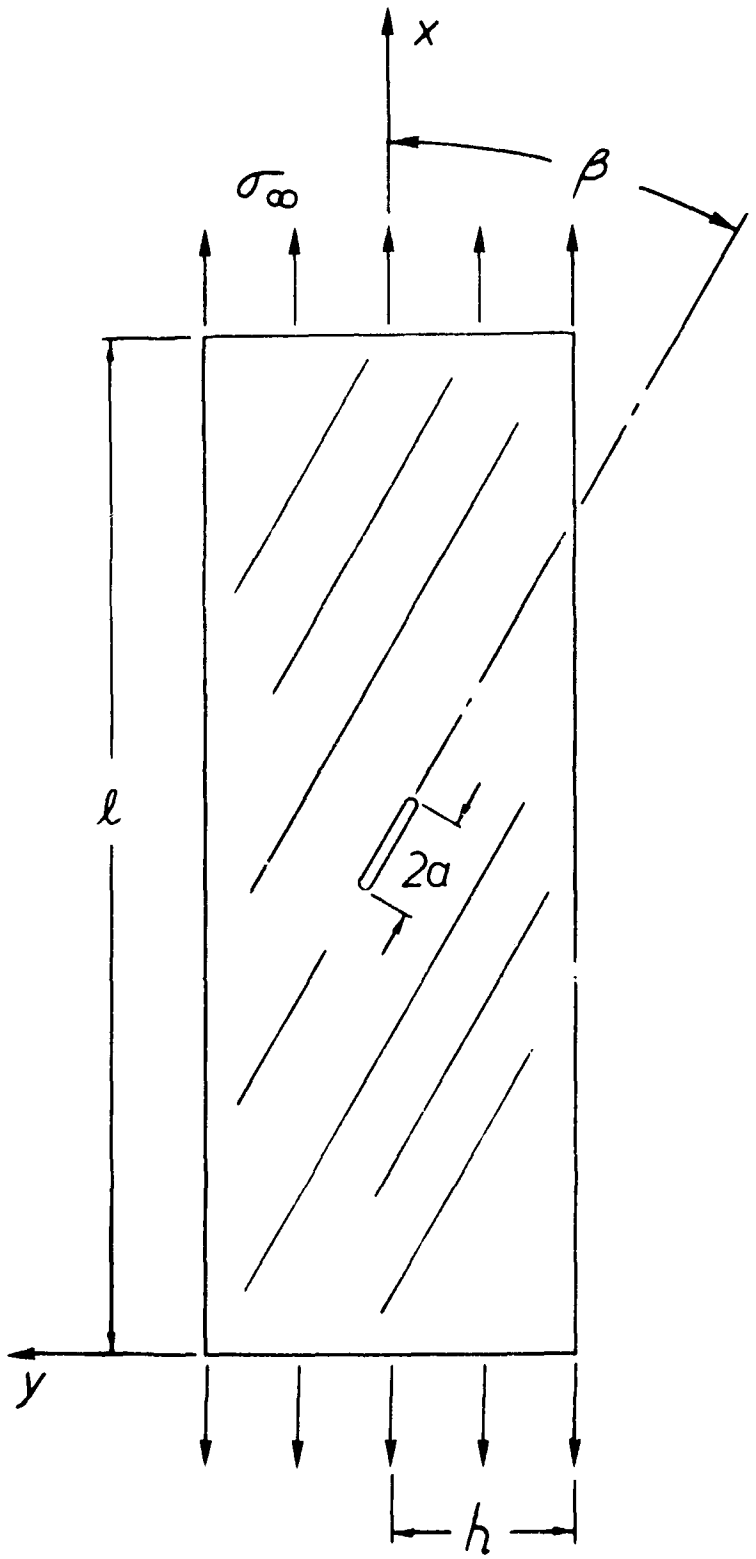


Figure 1. Unidirectional, Notched Off-axis Specimen Configuration

edge of the specimen buckled slightly as the crack closed. After the saw cut closed, the load picked up again, made up the lost 9% and failed at an additional 1%. The final stress-strain curve had an unusual "S" shape.

As the off-axis orientation angle, $\beta$, approaches zero in the off-axis tensile test, Figure 1, the Mode II component of crack tip forces also approaches zero. Another test configuration is therefore required to obtain the pure Mode II properties. A modified three rail shear test was suggested by Whitney [4] and verified numerically by Lakshminarayana [5] using finite element techniques. Excellent test results were then obtained using the specimen as shown in Figure 2. The test consisted of a flat unidirectional panel, bolted between three rails. The side rails are fixed, the center rail is movable and is loaded vertically downward, thus producing a state of in-plane shear in the two unclamped specimen areas. Exact specimen and fixture dimensions can be found in Reference 6. This test was originally used as a method to characterize in-plane shear modulus and strength. However, Mode II values can be determined by orienting the fibers parallel to the y-axis, then adding a notch at the center of the unclamped region, parallel to the fiber direction. Notches in the experimental program were cut and sharpened as described in the off-axis tensile test. The data presented was taken using the configuration shown in Figure 2, with the notch in the center of one open area and strain gages in the opposite area. Absolute symmetry, however, would be guaranteed if both areas were notched. Total cracks lengths of 5.08 mm (0.2 in) were used on T300/1034C specimens. A 25.4 mm (1 in) crack was required for the PEEK specimens to avoid premature transverse tensile failure.

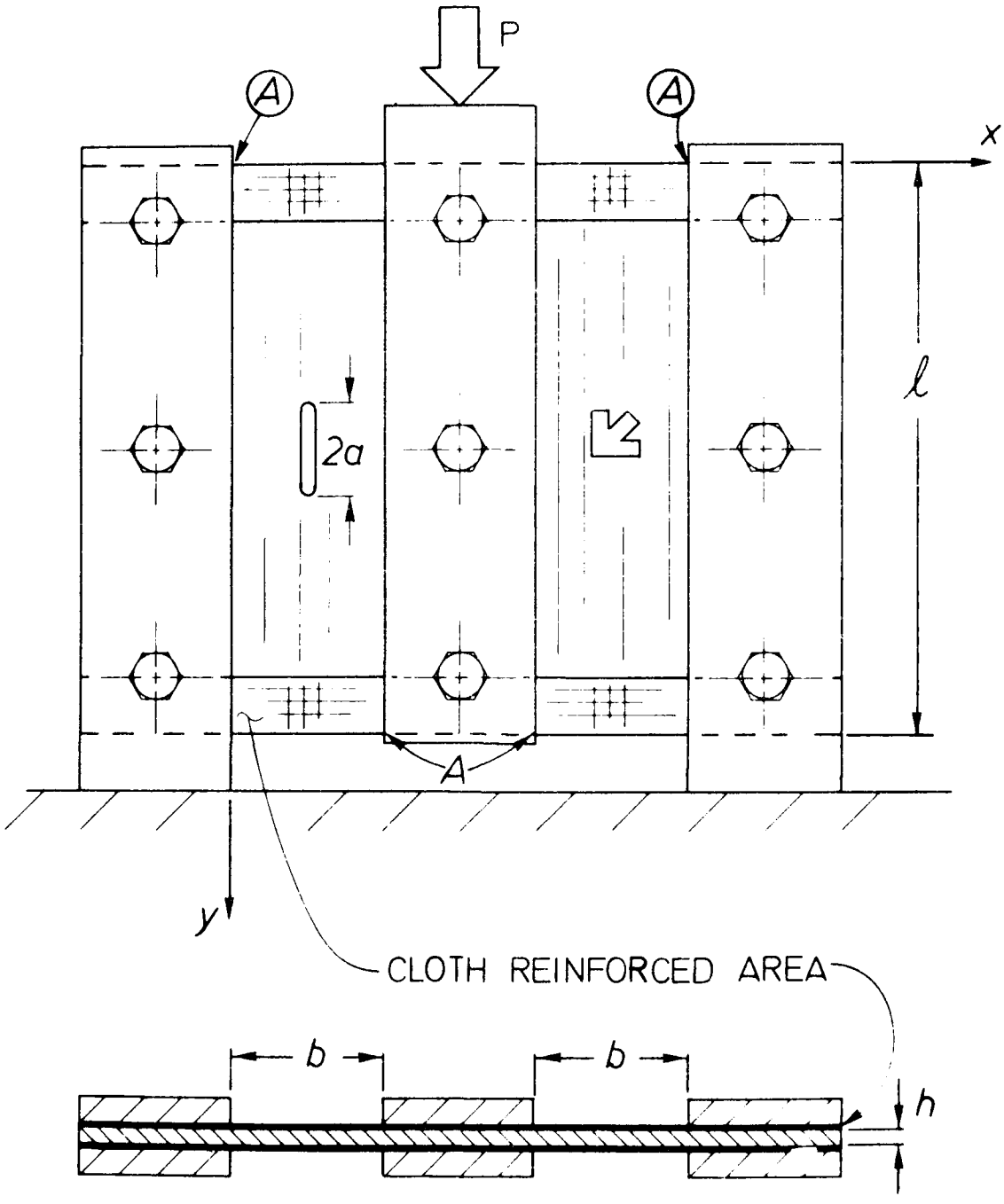


Figure 2. Modified Three Rail Shear Test for Determining $G_{IIc}$. Note Upper and Lower Edges are Reinforced to Prevent Premature Failure at the Edges

## SECTION III

## TEST RESULTS

Material toughness, given in terms of stress intensity factors, for the two material systems are plotted in Figure 3. Note the increased toughness of the thermoplastic system over the reinforced epoxy system. It is hoped the fracture surfaces may provide some explanation for this.

The unusually high Mode II for the APC-1 may be an artifact of the test (a much longer crack length was required to induce failure). A $K_{II_c}$ valve of about 6.5 MPa $\sqrt{m}$ would be consistent with the mixed-mode data shown in the figure.

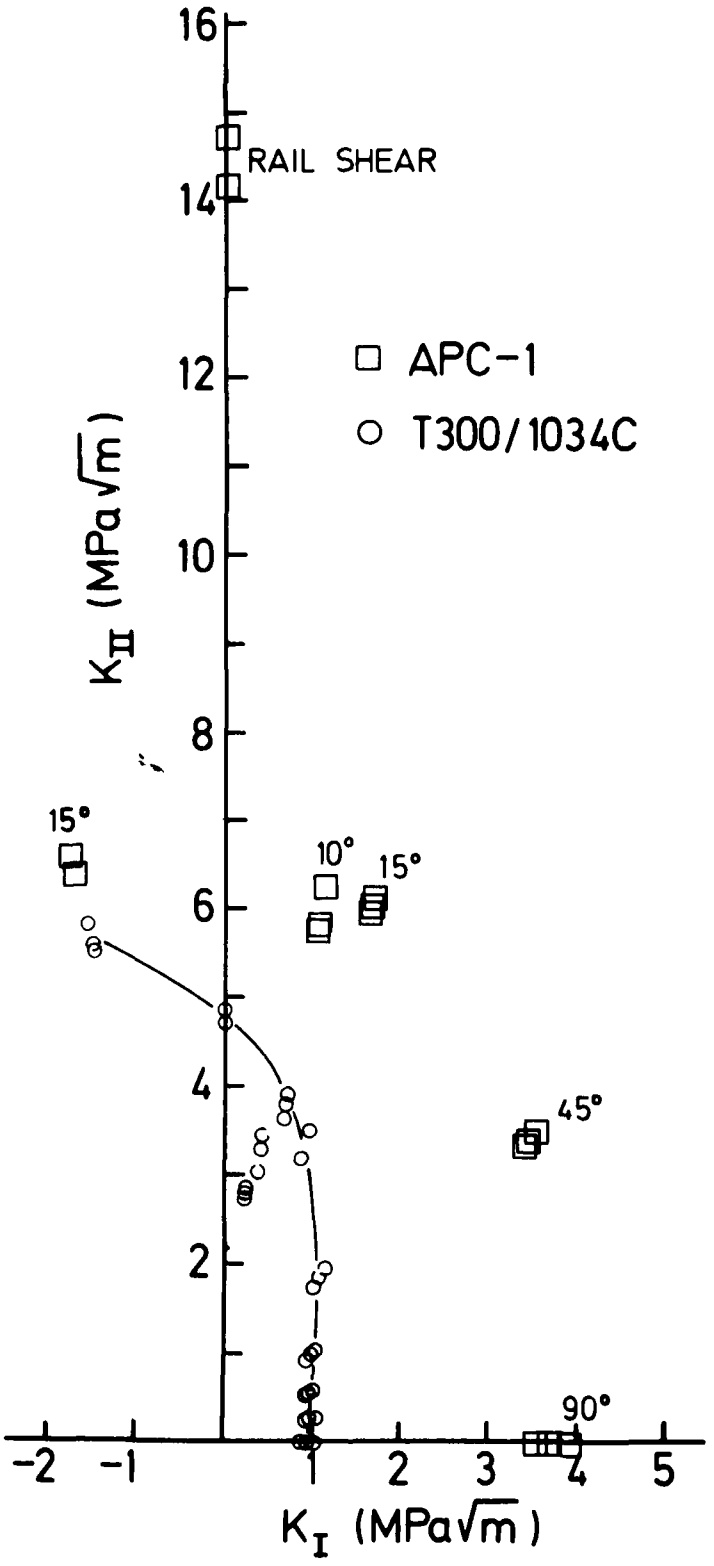


Figure 3. Mode II vs Mode I Critical Stress Intensity Factors for T300/1034C and APC-1 PEEK

## SECTION IV

## FRACTOGRAPHY PREPARATION

Sections near the crack tip of selected specimens were cut out, mounted, and gold coated for scanning electron microscope examination. Immediately before gold coating and before inserting the specimens in the microscope, the specimens were dusted using a can of compressed photographer's air. Therefore all debris seen on the surfaces were well adhered to the surface and are not due to dust or other contamination. All specimens were photographed at an angle of 30 degrees off the normal from each surface.

## SECTION V

## CRACK TIP STRESSES

The orientation of the fracture sections with respect to the overall specimen geometry was carefully noted when mounting the fracture surfaces. This is because the surface orientation determines the sign of the shear component in the non-ninety degree specimens.

The fracture morphology depends on the state of stress near the crack tip and the response of the fiber/matrix system to these stresses. The graphite/epoxy material provides a straight-forward opportunity to examine these stresses and how they correspond to the appearance of the actual fracture surface. The epoxy is a brittle material and will be assumed to fail due to large principal tensile opening stresses. All further discussion regarding failure in this section will be for the epoxy system. The descriptions of stress, however, are general and apply to the PEEK composites as well.

The quantitative description of the stress state ahead of the crack is complicated by such factors as crack tip damage, crack singularities, material anisotropy, and fiber spacing. Qualitatively, however, the stresses are simple to trace.

Figure 4 shows a crack advancing between fibers towards point A. Point A will experience normal and shear stresses due to the global stresses and due to the presence of the crack. These stresses can be transformed into their principal, shear free components. This principal orientation (1'-2') is at an angle $\theta$ with respect to the fiber-fixed (1-2) system.

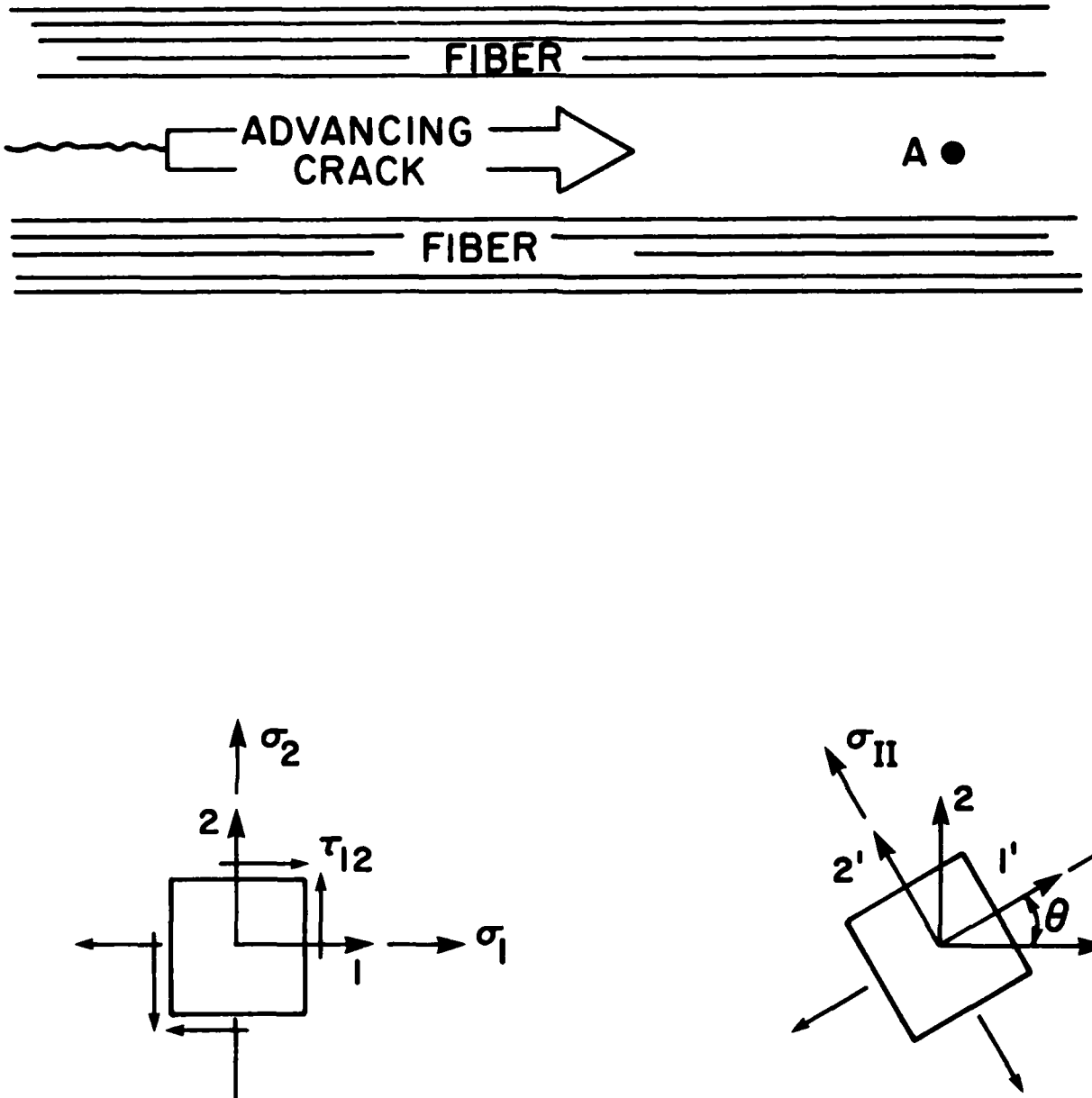


Figure 4. Stress State in Matrix at a Point Ahead of the Crack Tip

The Mode I case is depicted in Figure 5(a). The first column represents the stresses in the fiber-fixed co-ordinate system. In this case there is only $\sigma_2$. The next column shows the standard Mohr's circle depiction of the stress transformation from the fiber-fixed co-ordinates (shown as a heavy dot) into the principal components $\sigma_I$ and $\sigma_{II}$. All stress states are rotated from the fiber-fixed stresses (1-2 axes) to a state where $\sigma_I > 0$ (1'-2' axes). The 180° clockwise rotation to the principal axes on the Mohr's circle corresponds to a 90° counter-clockwise rotation for a positive $\sigma_I$. The tensile $\sigma_I$ is assumed to cause local matrix fracture due to its brittle nature. Therefore, the fracture plane should be normal to the 1' axes. In this trivial example, the 2 and 1' axes correspond, as expected. Physically, the crack should proceed cleanly and easily through the matrix between fibers.

The addition of shearing forces with the opening forces are depicted in Figures 5(b) and 5(c). It can be seen that the principal tensile forces act at an angle with respect to the fibers. The closer point A in Figure 4 is to the crack front, the higher the magnitude of these stresses due to the crack singularity effect. The result, then, is a series of angled cracks, between fibers, ahead of the crack itself. Researchers such as Purslow [7], Bradley [8], and Davidovitz [9] have observed these angled cracks ahead of the main crack. As the main crack progresses forward, the material left between these smaller cracks remains attached to the split surfaces. These remaining pieces are the hackle formations seen in failures involving shear [10]. A reversal of the direction of the shear load reverses the orientation of the hackle tilt, shown as the difference between Figures 5(b) and 5(c).

The removal of the tensile opening load, leaving only the shear load, is shown in Figures 5(d) and 5(e). The hackles should form at 45°.

As shown in Figures 5(f) and 5(g), compressive, or crack closing forces, combined with shear should cause the hackles to "raise up".

These trends can be related to the test methods shown in Figures 1 and 2, and, it is hoped, ultimately to the appearance of the fracture surfaces. When $\beta = 90$ (Figure 1), the area forward of the crack experiences stresses as shown in Figure 5(a). A continuous crack should occur, as explained previously. As $\beta$ becomes less than 90°, the state-of-stress in Figure 5(c) results. The hackles should be laying nearly flat. As $\beta$ approaches zero, the hackles should progressively raise to nearly 45°.

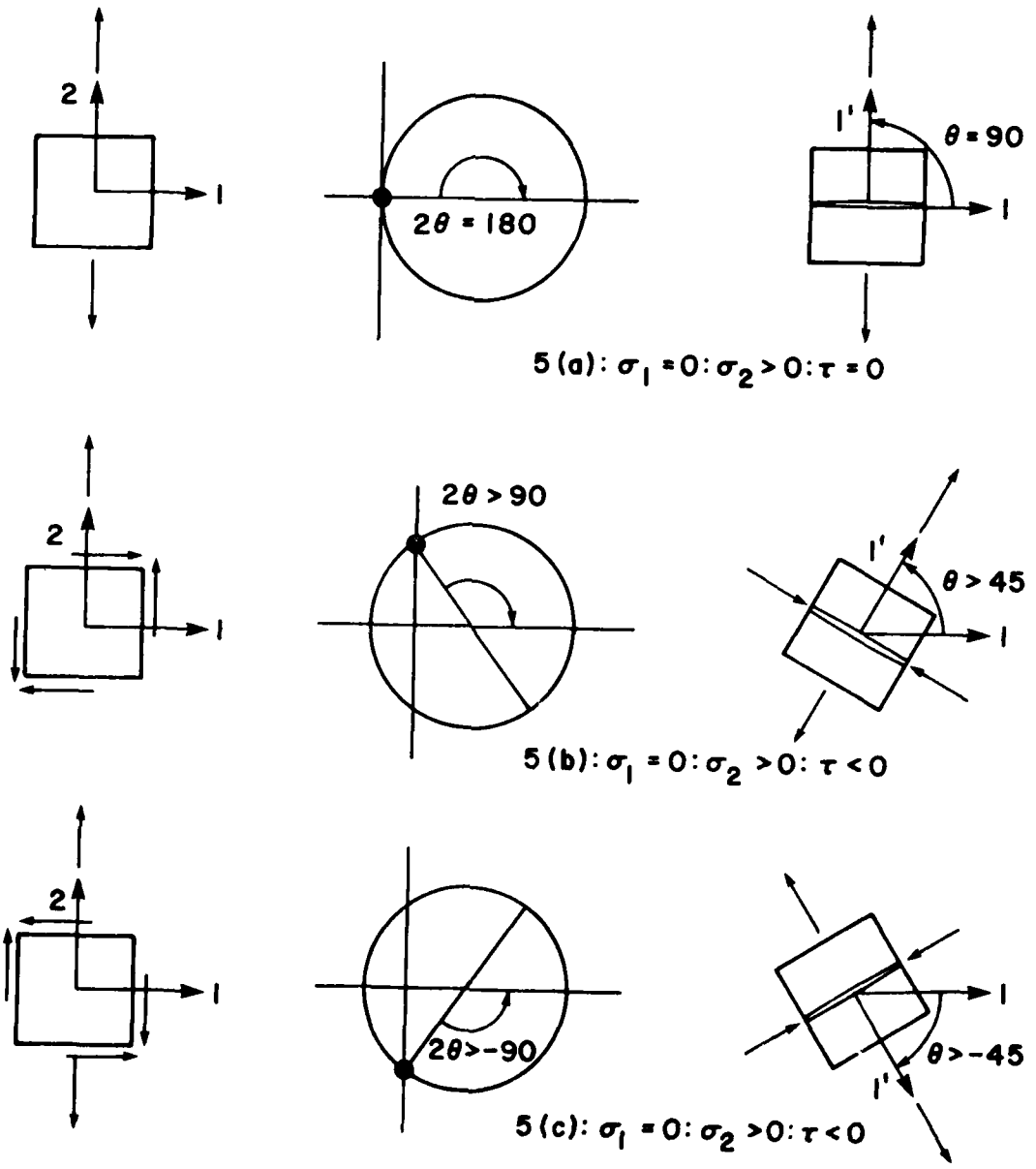


Figure 5. Various Combinations of Stress Ahead of the Crack. The Left Column Represents the Stresses in the Fiber-Fixed Co-ordinates, the Center Column the Mohr's Circle Representation of these Stresses, the Right Column the Stresses at their Principal Orientation. Positive Angular Rotations to the Principal Axes are Clockwise When Shown on the Mohr's Circle, Counter-Clockwise on the Physical Representation (The Third Column). The Cracks Drawn in the Third Column Represent the Orientation the Hackle-Forming Cracks would be if Produced by the Tensile Principal Stress Component (Brittle Material Behavior).

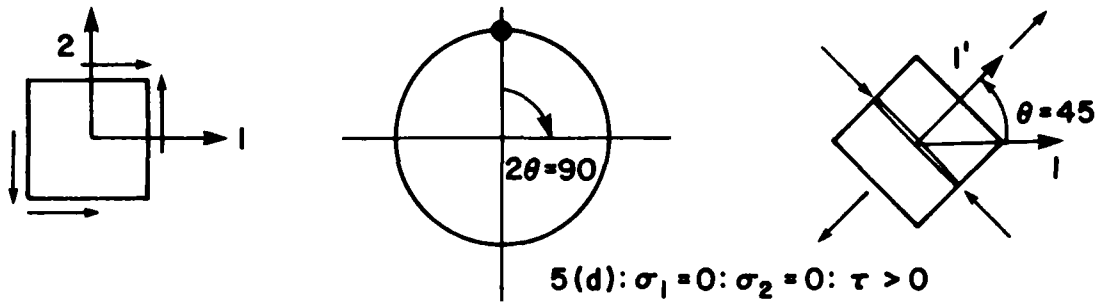


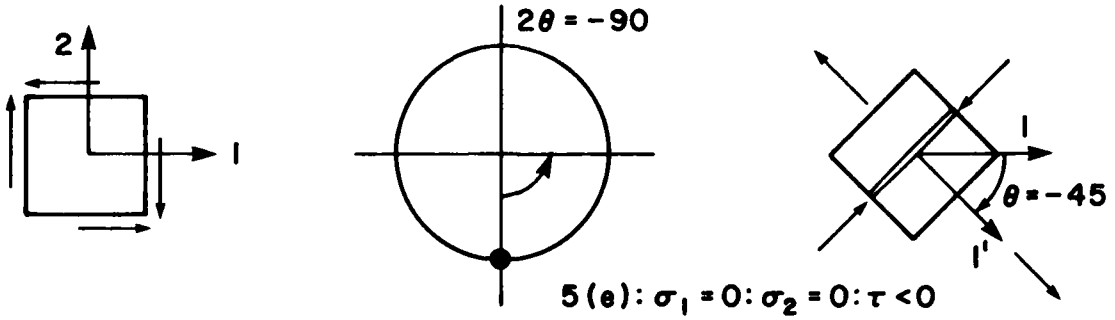


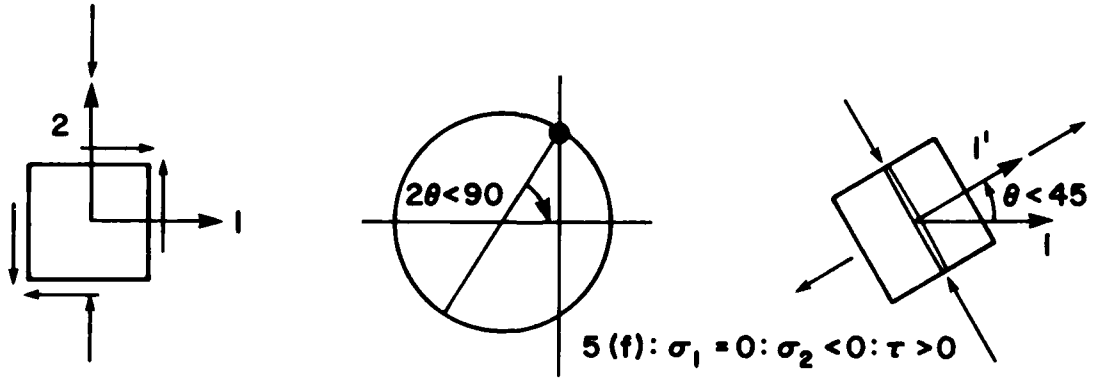


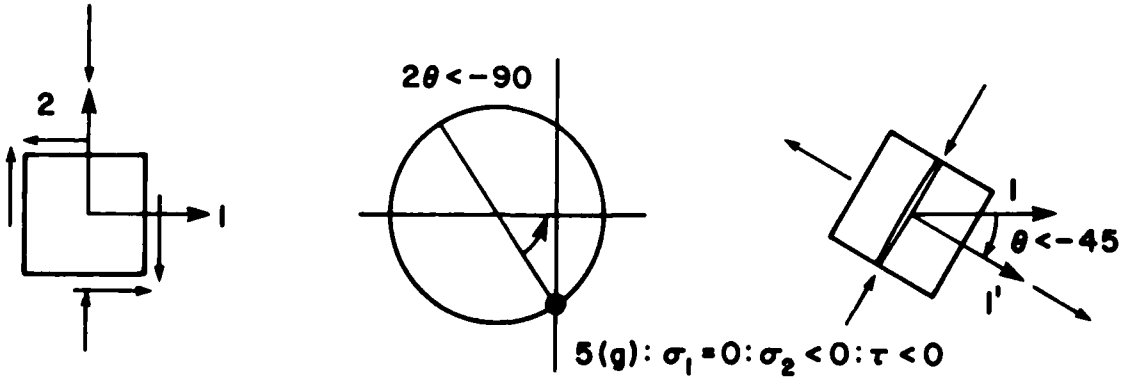


Figure 5 (Concluded)

## SECTION VI

## PHOTOGRAPHS

The photographs in this section are divided into two main groups: the graphite/epoxy and the graphite/PEEK specimens. Within each of these groups are four photos of each specimen. The first two photos are the low magnification (100X) shots. This magnification is useful for observing the amount and direction of fiber breakage, the amount and direction of fiber or fiber group pull-up, the amount of irregularity in the cross section, and the amount of debris. Since the specimens were center-notched, four fracture surfaces result from the failure: top and bottom, left and right, depicted as surfaces A and B in Figure 6. Note that in surfaces A and B the direction of shear is the same, but the crack direction is different (right to left in A, left to right in B). The low magnification shots show a smooth area corresponding to the saw cut, then a narrow band that was the razor-sharpening.

The second two photos of each section are 800X. These provide useful information such as the pattern of matrix fracture, the look of the broken fiber ends, and the amount of resin debris.

Photographs of off-axis specimens, graphite/epoxy only, and not including the rail shear surface, are given in References 10 and 11.

1. GRAPHITE/EPOXY

Figure 8, $\beta = 90°$, $K_I$ only.

The 800X views show the matrix has failed in a smooth cleavage fashion. Very many long matrix wedges are visible. These result from the resin areas between fibers. (See Figure 7).

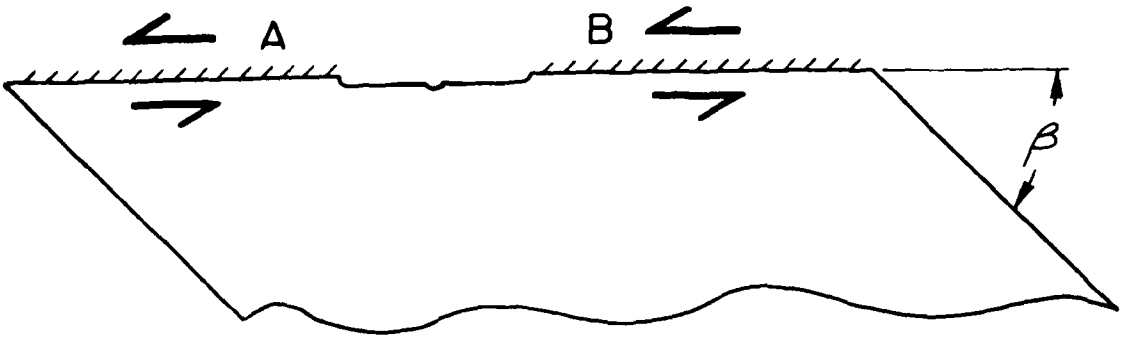


Figure 6. One-half of Fractured Specimen with Shear Forces and Hackle Direction Noted

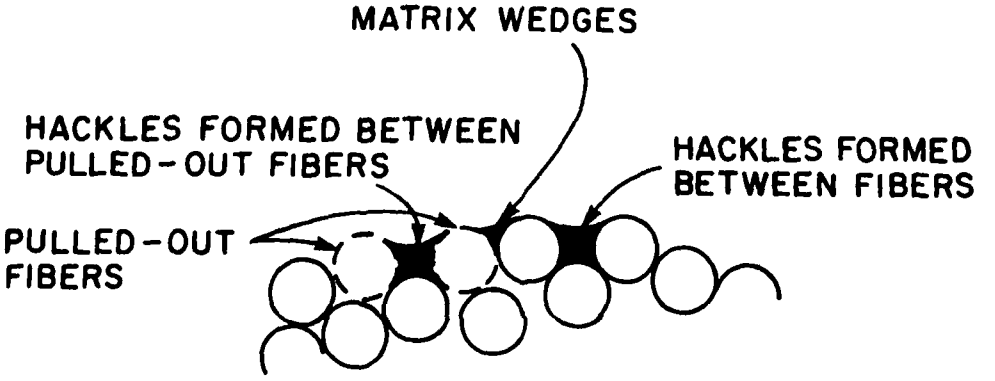


Figure 7. Cross-Section of Fracture Surface. Top Part is the Actual Fractured Surface Area. Drawing Shows where Wedges and Hackles Form in the Matrix Areas

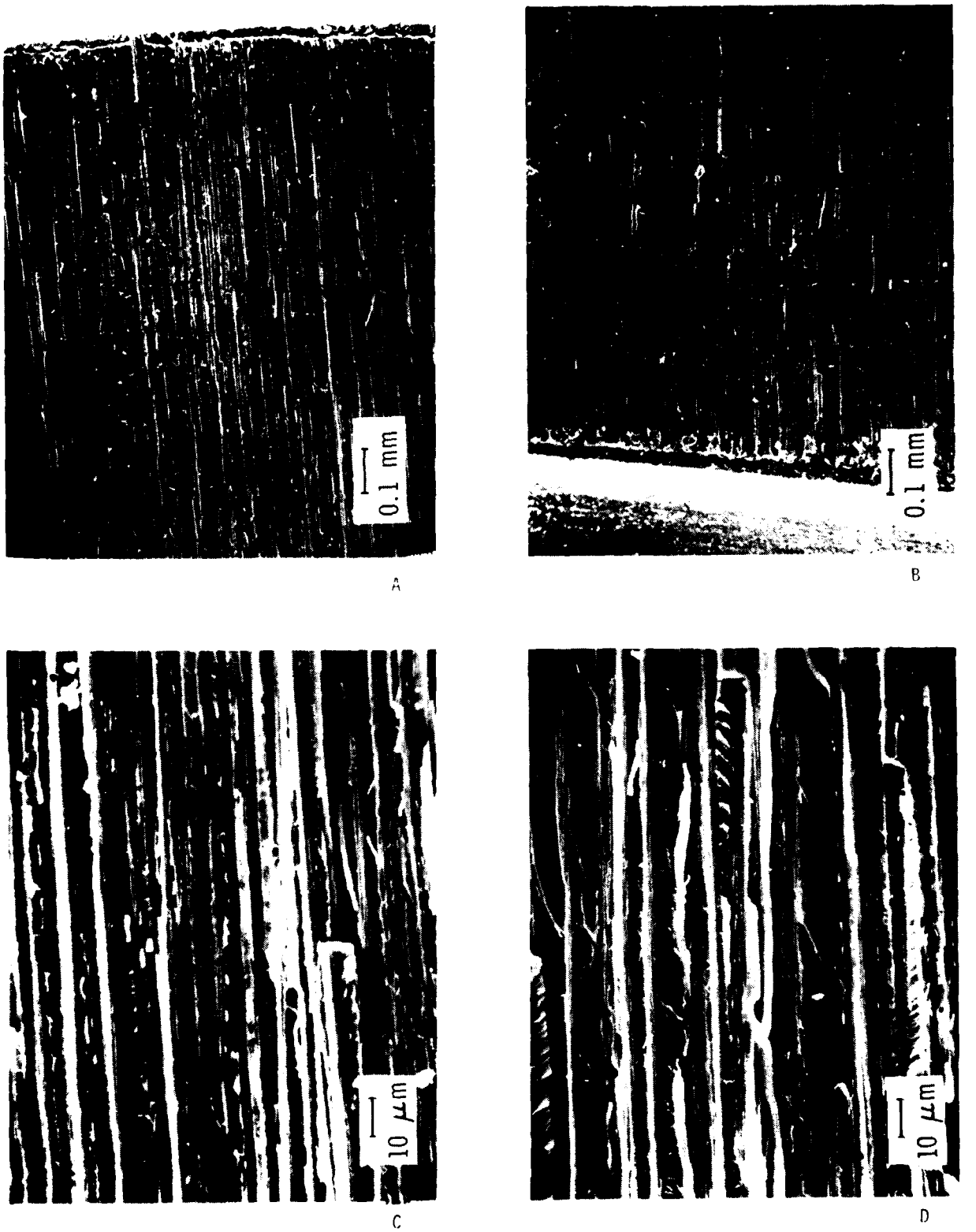


Figure 8. Beta = 90 deg, $K_I$ Only. T300/1034c

Note the clean fiber breaks. Some matrix lacerations, or hackles as they are sometimes called, are seen in the grooves of the missing fibers. These are likely due to local shearing along the side walls of the fiber as it was pulled away.

Figure 9, $\beta = 45°$, $K_I/K_{II} = 1.0$.

The 100X magnification shows a roughly equivalent number of fiber breaks in each direction on each surface. The first 800X photo (9c) shows a large number of fairly small hackles, evenly spaced and lying nearly flat. Matrix wedges are still visible. There were some bands with no hackles, as shown in Figure 9(d). Note the hackles form in the resin areas between fibers, as depicted in Figure 7. The fibers boardering the hackles may still be in place, 9(d), or missing, 9(c).

Figure 10, $\beta = 30°$, $K_I/K_{II} = 0.58$.

The 100X photos show there are still many broken fibers in both directions, although there are more pointing to the left. Figure 6 shows that fibers on both surfaces experience a force to the left due to the global shear force. If the fibers break more easily in tension than compression, one would indeed expect more broken fibers pointing left. The 800X views show the hackles have become more raised than in the 45° specimen, as expected in the discussion earlier. Also visible are large hackles, formed in an area with more space between fibers.

Figure 11, $\beta = 15°$, $K_I/K_{II} = 0.27$.

By now, nearly all of the fiber breaks point left, as shown in the 100X photos. The 800X shows the hackles are nearly vertical - more than expected from the stress analysis. Their spacing has become very irregular. The fiber breaks clearly show the effects of shear direction. Broken fibers pointing to the left have failed in tension. Broken fibers

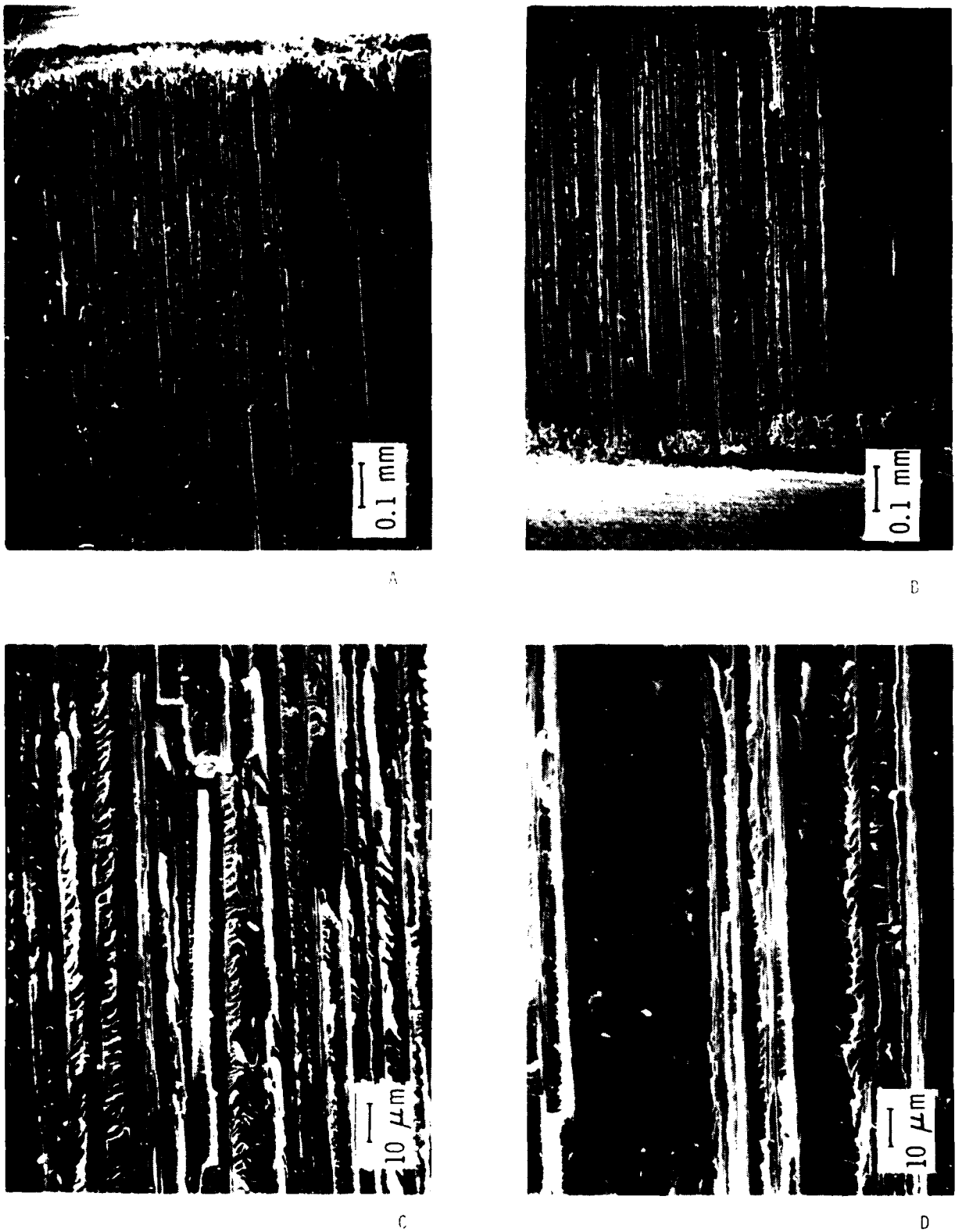


Figure 9. Beta = 45 deg, $K_I/K_{II}$ = 1.0, T300/1034c

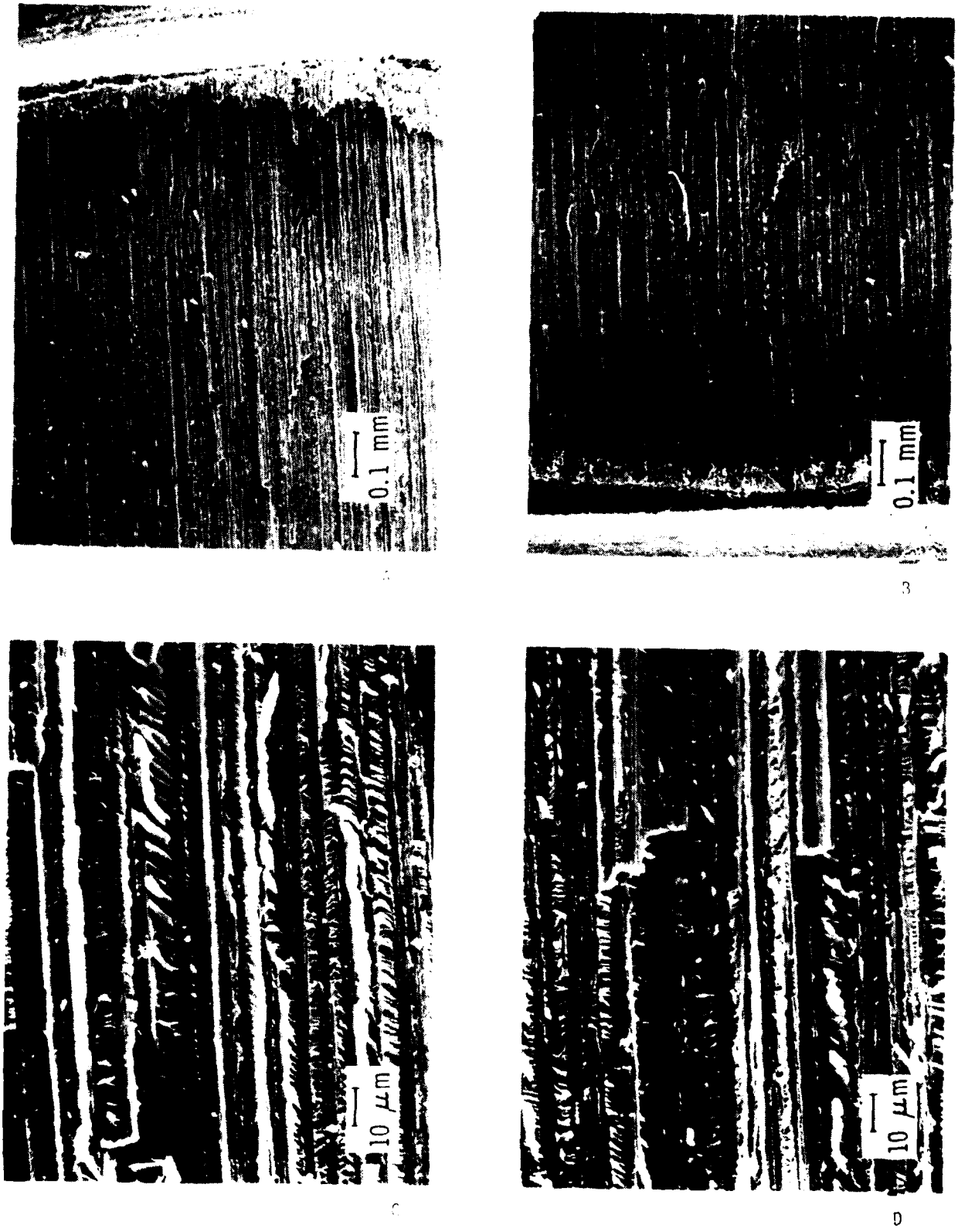


Figure 10. Setup [illegible] deg, $E_1/E_{11}$ = 0.58. T300/1034c

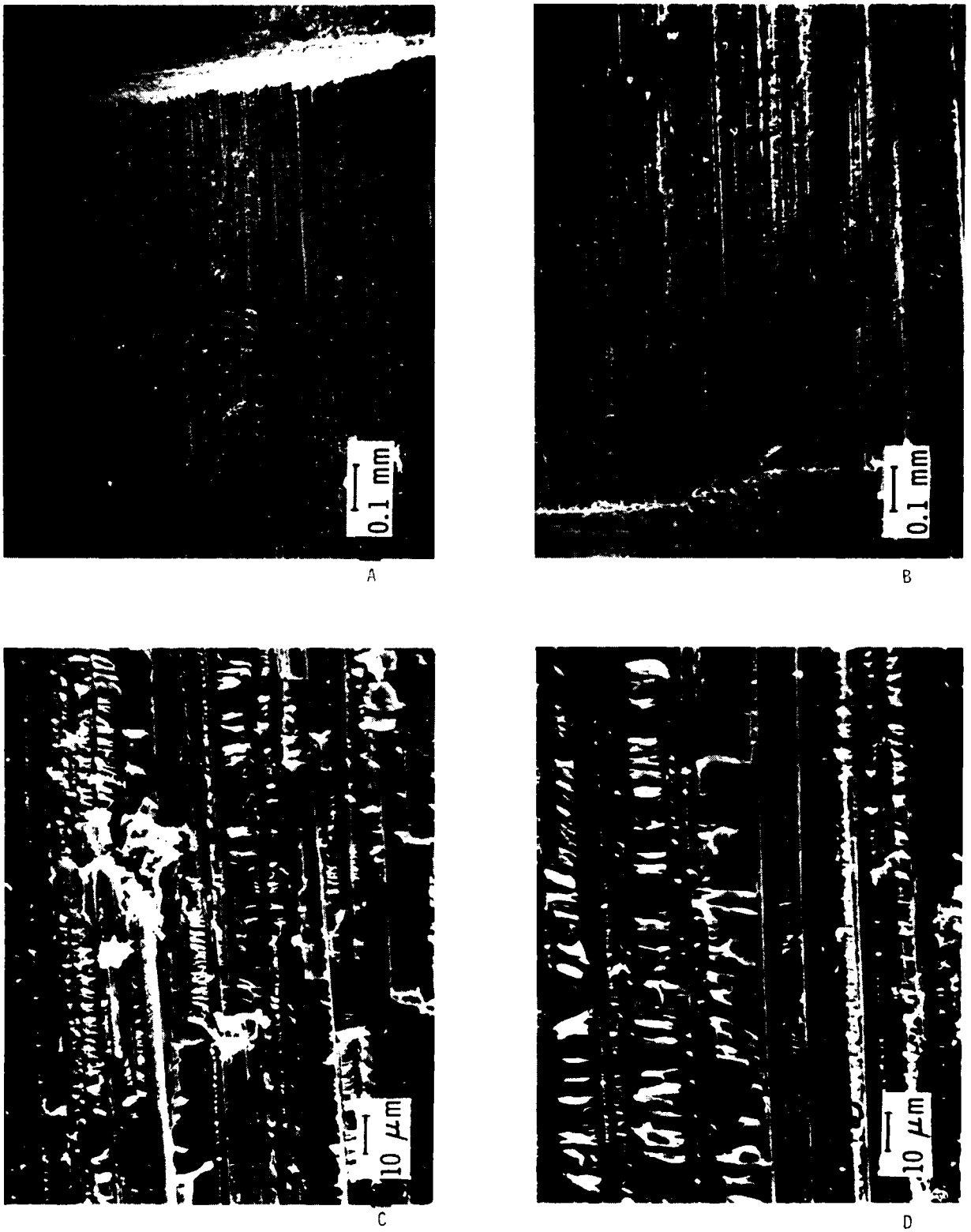


Figure 11. Beta = 15 deg, $K_I/K_{II}$ = 0.27. T300/1034c

pointing to the right show a compression mushrooming type of failure. An increase in resin debris, as reported by Hahn and Johannesson [11] is apparent.

Figure 12, $\beta = 10°$, $K_I/K_{II} = 0.18$.

Fibers broken in tension, 12(d), and compression, 12(c), clearly show shear direction. The hackle spacing is more irregular.

Figure 13, Rail Shear, $K_{II}$ only.

The fiber breaks continue their failure pattern. Some have even segmented and are wedged with resin debris, 13(d). The matrix hackles have become very block-like (they are referred to by Purslow [7] as cusps), and exist only in the deep crevices between fibers. Their spacing is very intermittent. Exposed fiber surfaces are stripped clean.

Figure 14, $\beta = 15°$ compression, $K_I/K_{II} = -0.27$.

In these photos, the shear direction is opposite to that shown in Figure 6. Note the large amount of resin debris remaining on the surface. Some areas, 14(c), show segmented fibers. The surface has a general ground down appearance, as expected due to friction between the upper and lower surfaces during fracture.

In general, the 90 degree fracture surface remained very planar from the saw cut to the specimen edge. As the $K_{II}$ component increased, however, the surfaces became increasingly more irregular in cross-section. The increase in hackle formation, resin debris, and surface roughness obviously requires more energy than the clean Mode I cleavage fracture. This accounts for the much higher toughness as Mode II loading is introduced. Another interesting point is that surfaces A and B, as shown in Figure 6, both have the same general appearance for a

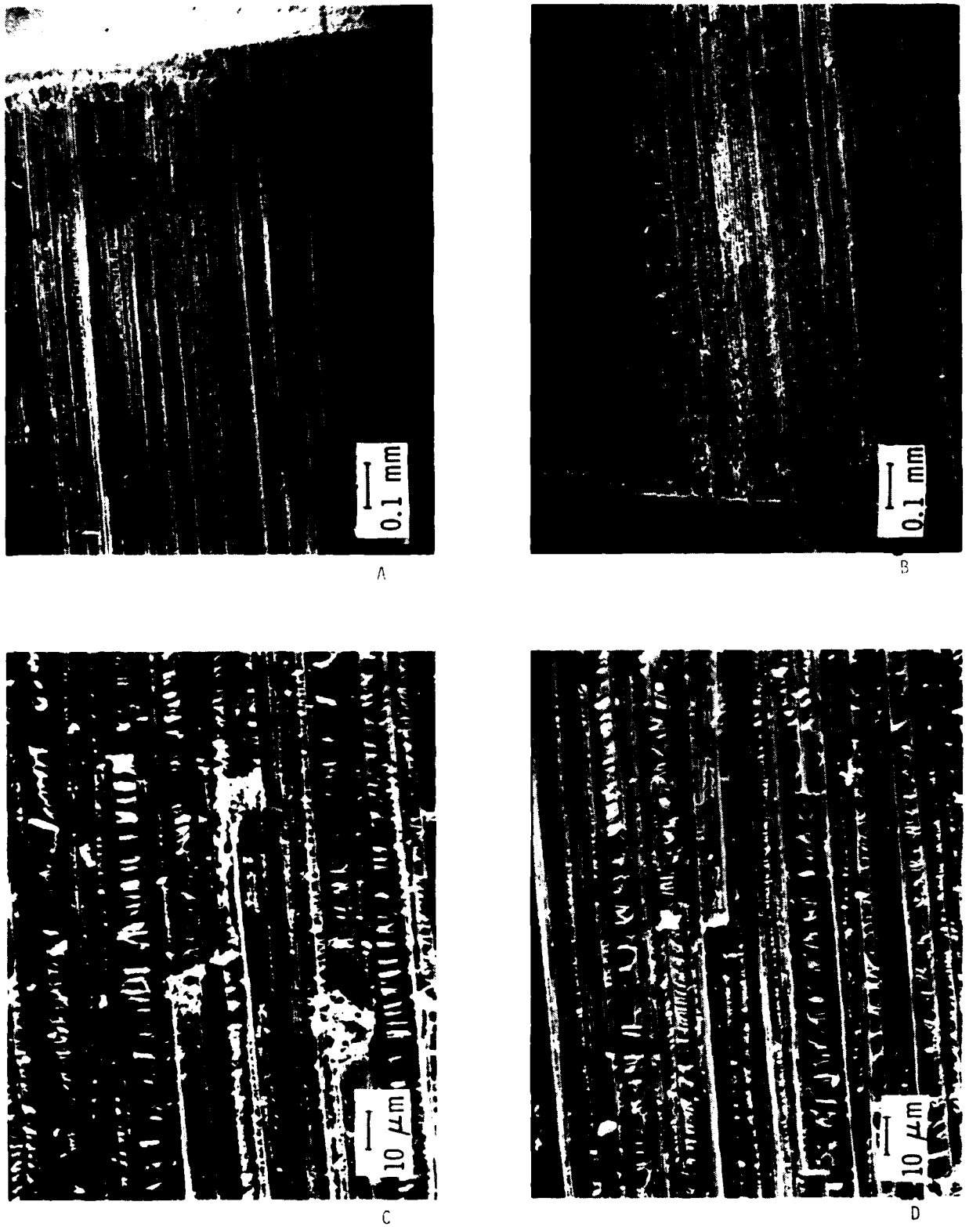


Figure 17. Beta = 10 deg, $K_I/K_{II}$ = 0.18. T300/1034c

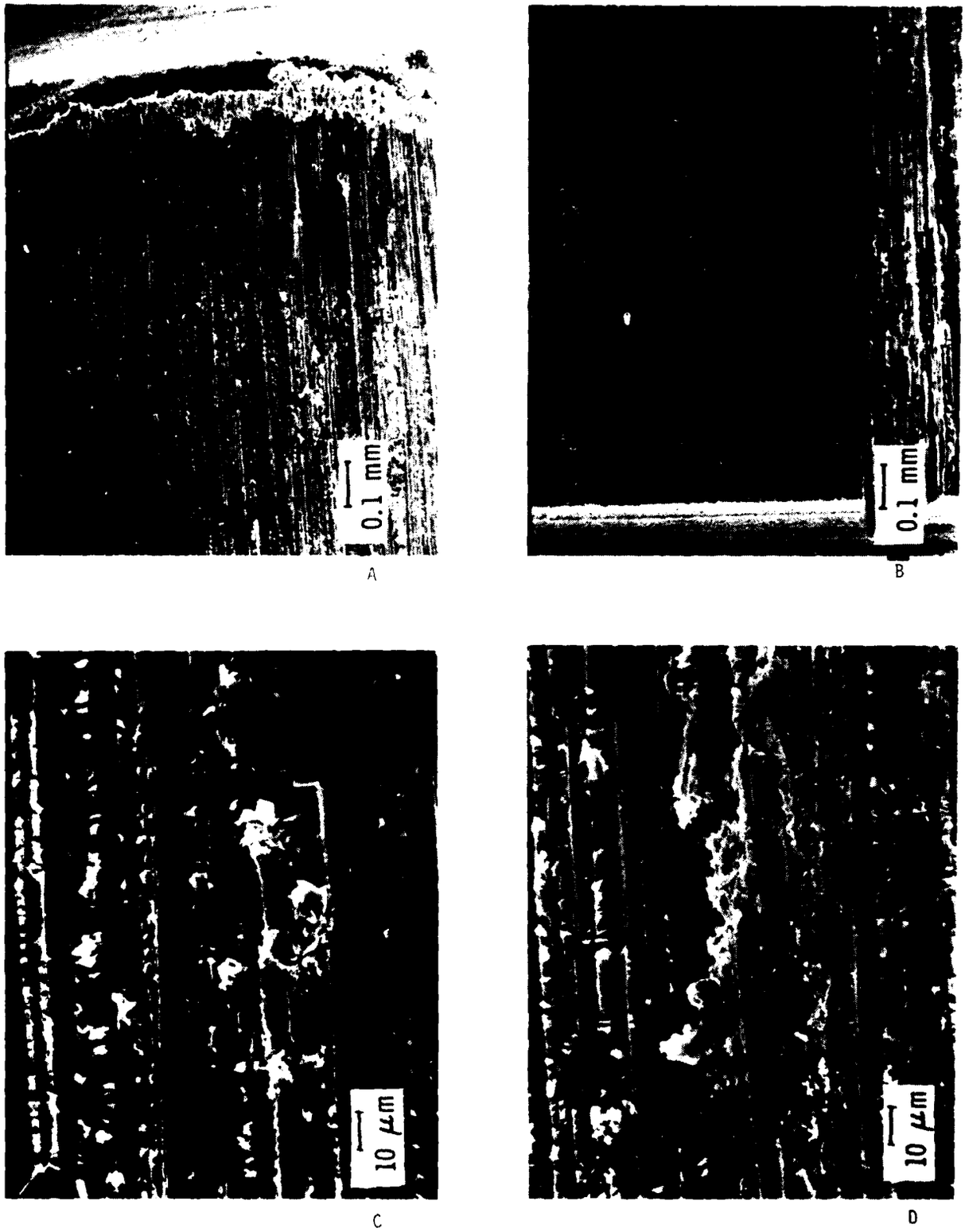


Figure 13. Rail Shear, $K_{II}$ Only. T300/1034c

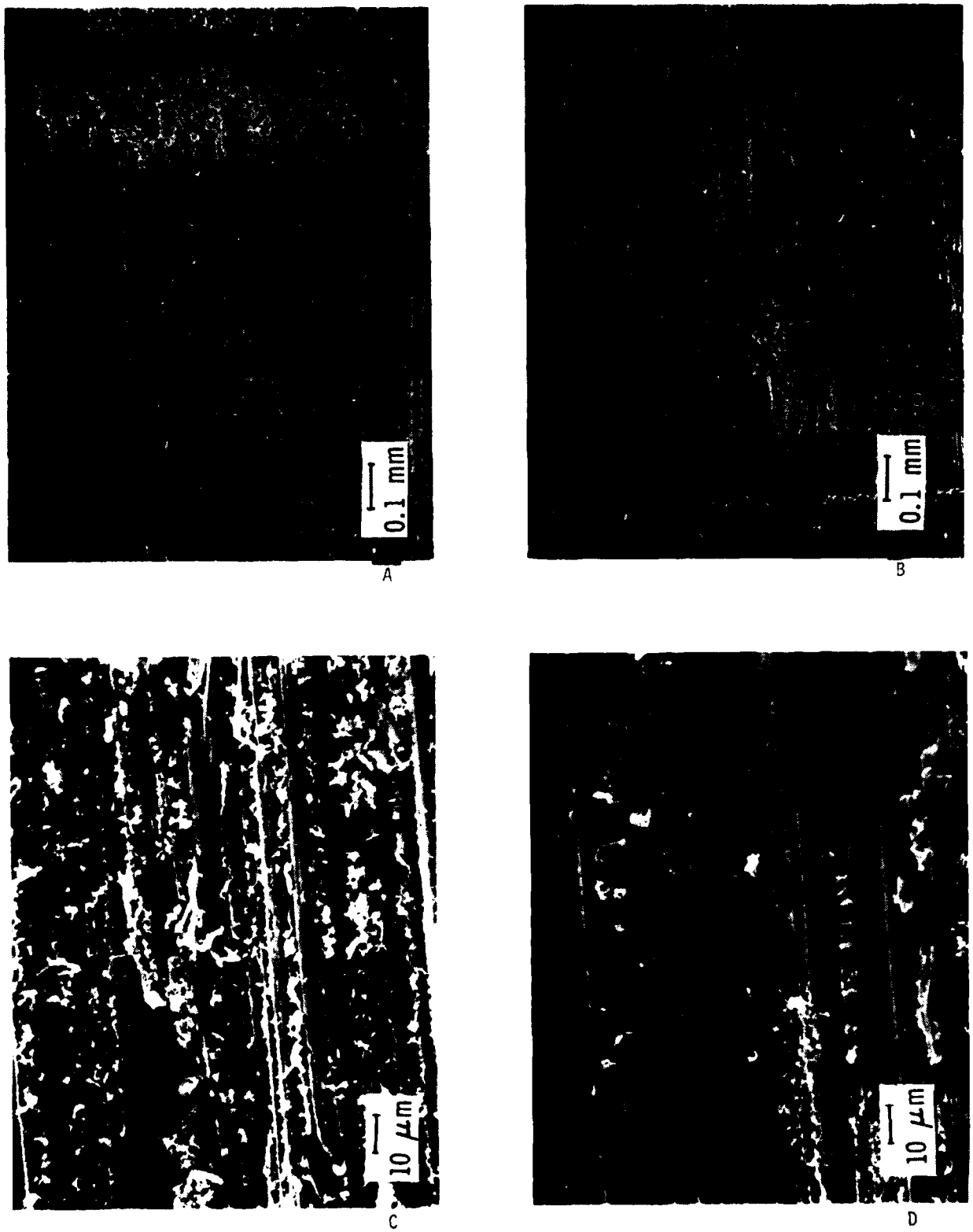


Figure 14. Beta = 15 deg Compression, $K_I/K_{II}$ = -0.27 T300/1034c

fixed orientation. Hackle direction and fiber breaks were identical, and were determined by the state of shear, which was the same in both surfaces. This investigation showed no evidence, except in the pure Mode I case, to indicate crack propagation direction (right to left in surface A, left to right in surface B), an important tool in post-mortem analysis.

2. GRAPHITE/PEEK

Figure 15, $\beta = 90°$, $K_I$ only.

Even at 100X it is obvious that much more energy went into the fracture than into the equivalent epoxy specimen. The surface is very uneven, and some groups of fibers have been pulled up. Higher magnification shows large amounts of resin adhered to the fibers.

Figure 16, $\beta = 45°$, $K_I/K_{II} = 1.0$.

The 100X photos show that most broken fibers point to the left on both surfaces. The 800X shots show rough, thick hackles. Figure 16(c) shows tensile, and 16(d), compressive evidence to show shear direction in the graphite/PEEK. This direction agrees with the hackle orientation.

Figure 17, $\beta = 15°$, $K_I/K_{II} = 0.27$.

A series of pointed spike formations are present in the region of the crack tip. Note they point in the direction of the applied shear stress. These spikes appear as though formed by crazing [12]: As the opposing fracture surfaces displaced under opening and shear forces, the spikes necked down in a ductile manner until they broke off at the mid-section.

Figure 18, $\beta = 10°$, $K_I/K_{II} = 0.18$.

The spike formations are still prevalent. Figure 18(c) shows tensile and compressive fiber failures. Figure 18(d) shows a rare feature found

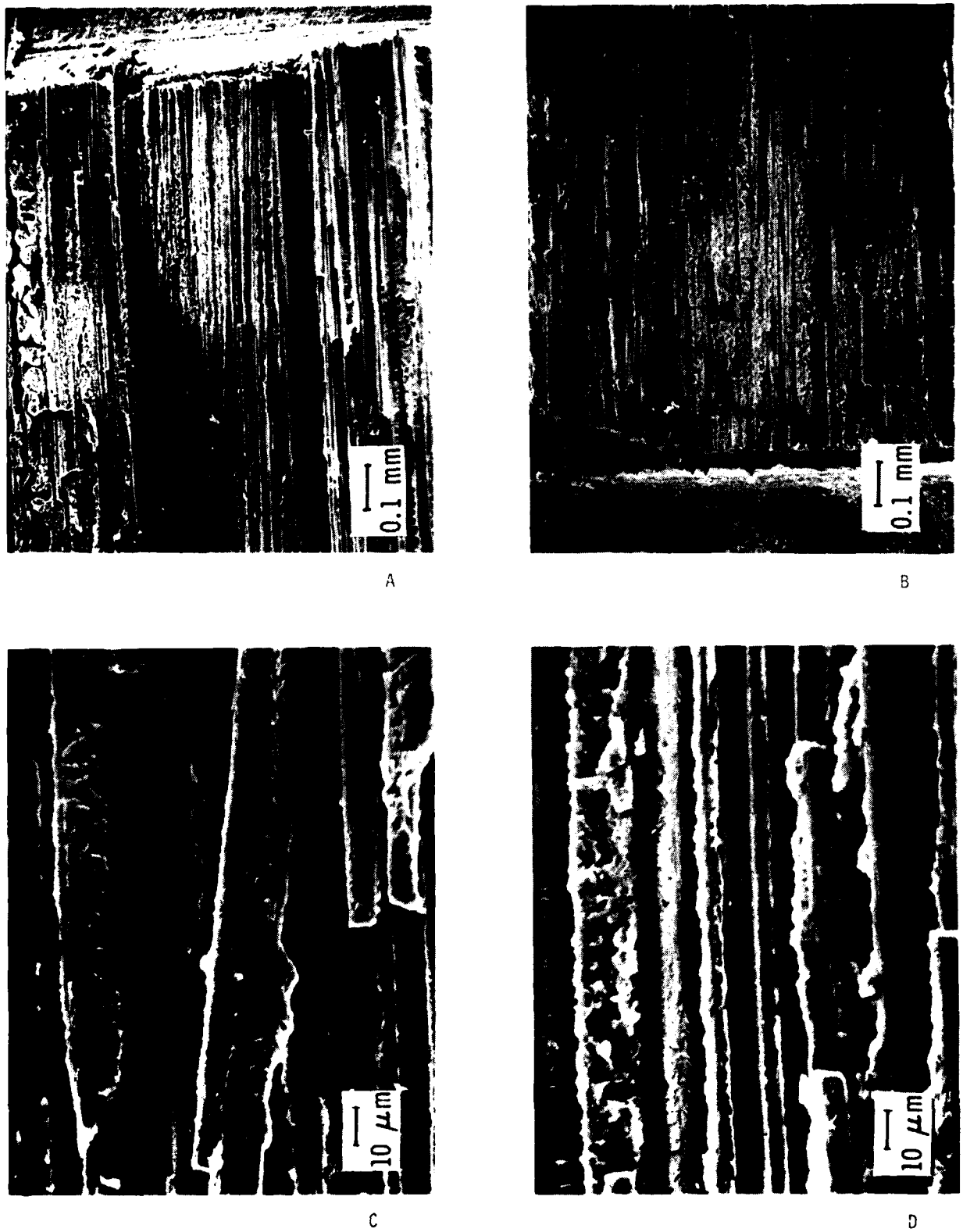


Figure 15. Beta = 90 deg. $K_I$ Only. APC-1

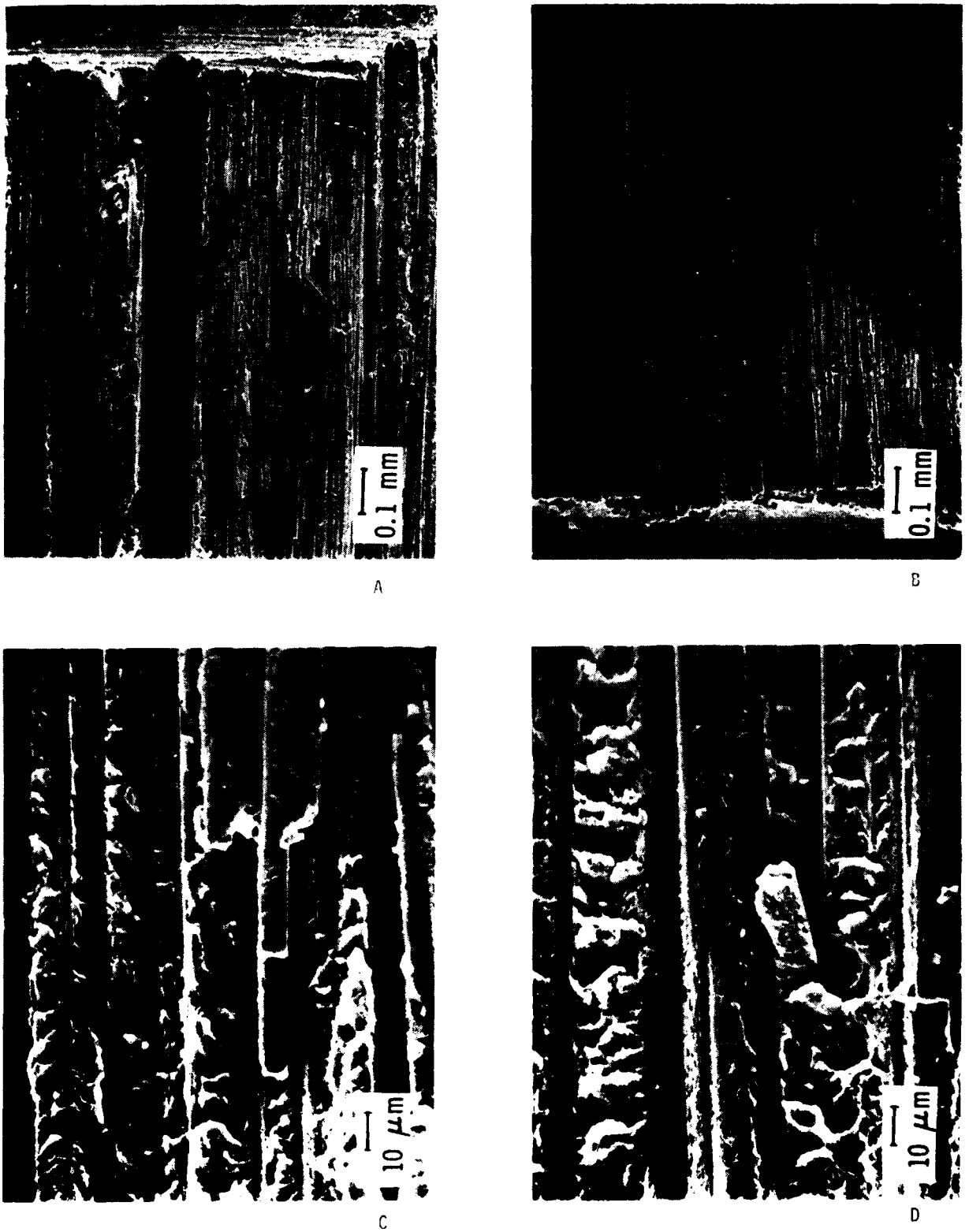


Figure 16. Beta = 45 deg, $K_I/K_{II}$ = 1.0. APC-1

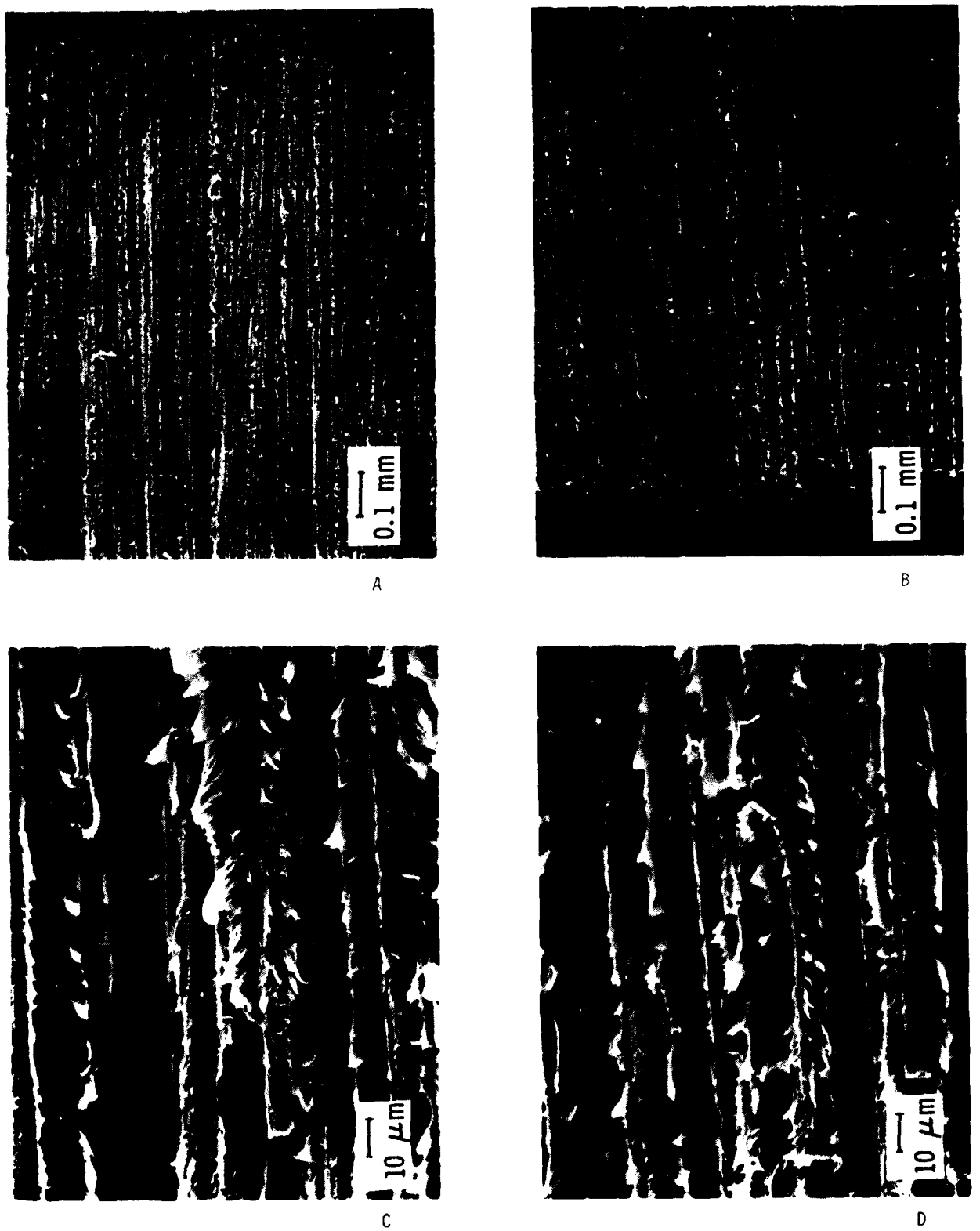


Figure 17. Beta = 15 deg, $K_I/K_{II}$ = 0.27. APC-1

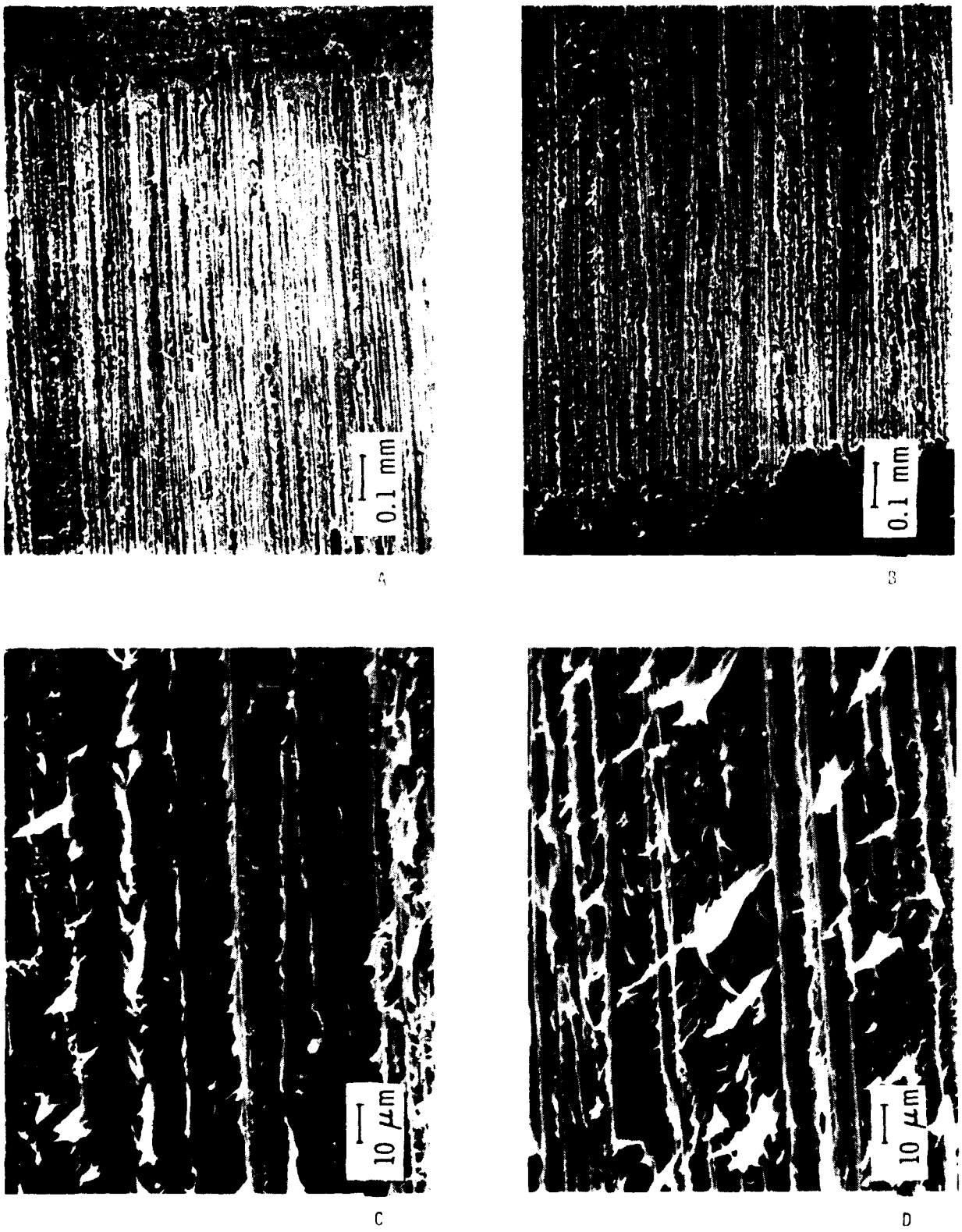


Figure 18. Beta = 10 deg, $K_I/K_{II}$ = 0.18. APC-1

on the surface: sheaths from around the fibers pulled-up almost cobra-like.

Figure 19, Rail Shear, $K_{II}$ only.

The spikes in Figure 19(c) are well developed and leaning strongly in the shear direction. Tensile and compressive fiber breaks can be seen in this photograph. There are also smooth bands on the fracture surface, shown in Figure 19(d) at 800X. Compressive fiber failures can be seen in this photo.

Figure 20, $\beta = 15°$ compression, $K_I/K_{II} = -0.27$.

The surface at 100X shows the specimen buckling that occurred in compression. The surface had several zones. One type, as shown in Figure 20(c), was mottled and had much debris. The second type was smoother and darker, 20(d).

In general, the graphite/PEEK specimens did not show as dramatic a change in surface morphology from 15° to rail shear as the graphite/epoxy showed. As with the epoxy, both left and right fracture surfaces (A and B in Figure 6) at each orientation looked similar, even though the crack propagation direction was different in each. The sign of the shear component of stress was responsible for the orientation of the surface features.

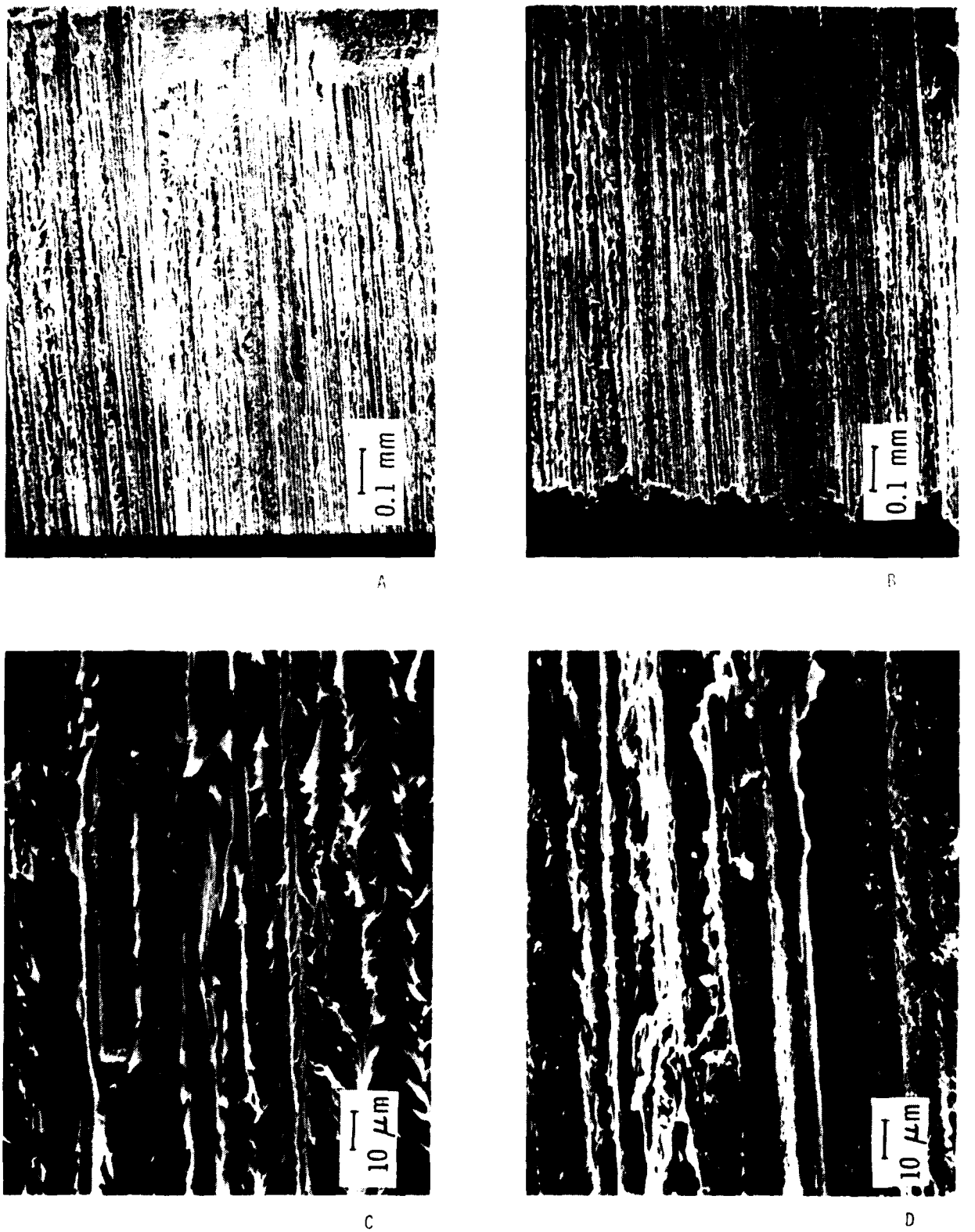


Figure 19. Rail Shear, $K_{II}$ Only. APC-1

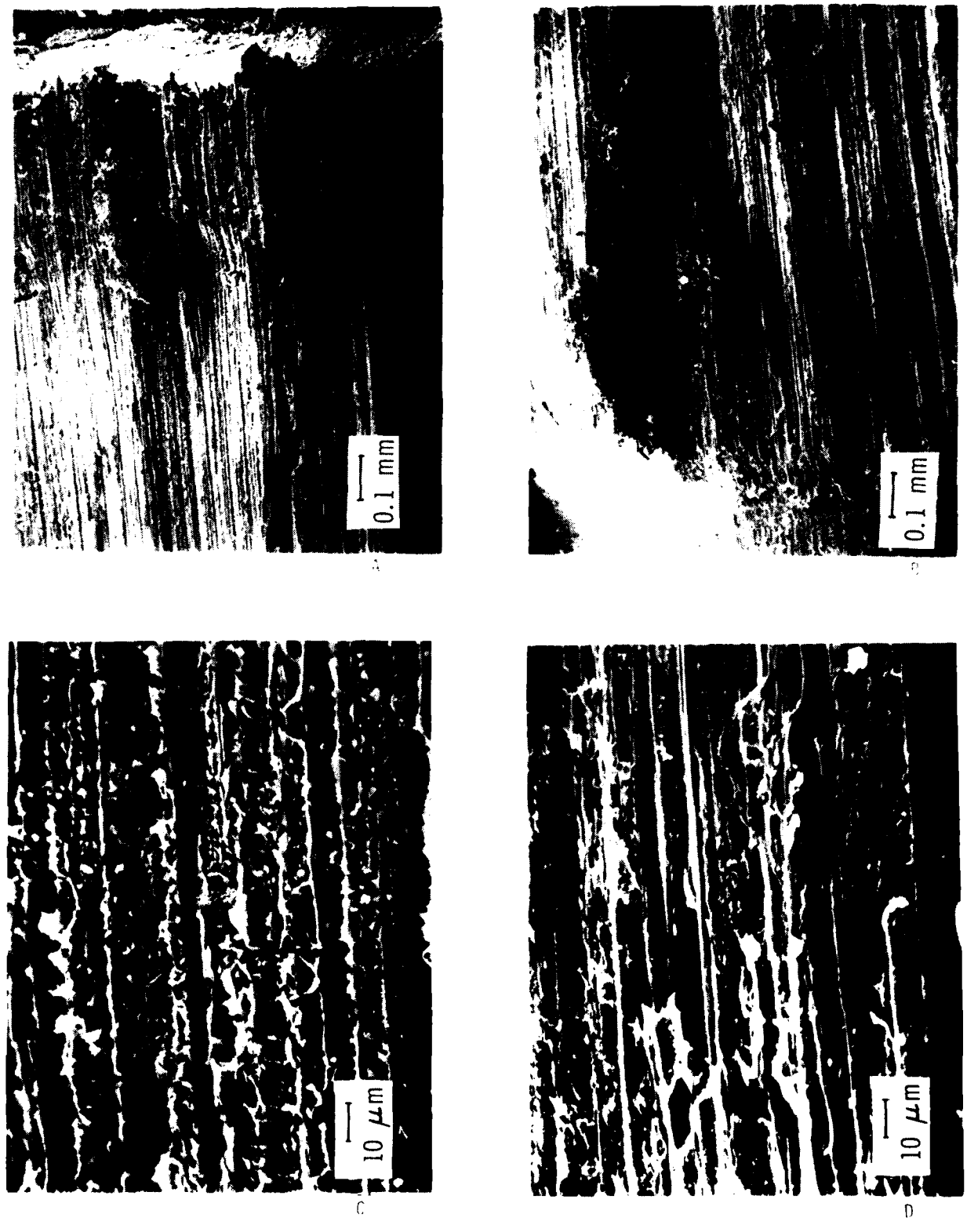


Figure 20. Beta = 15 deg Compression, $K_I/K_{II}$ = -0.27, APC-1

## SECTION VII

## CONCLUSIONS

The reason for the increased amount of energy required to fracture composite specimens under increased Mode II loading is clear upon examination of the fracture surfaces. In graphite/epoxy, increased shear loading leads to extensive matrix cracking between fibers, debris formation, compression fiber failure, and surface irregularity. In the thermoplastic, much ductile matrix deformation occurs. The more brittle epoxy and tougher thermoplastic showed very dissimilar fracture surfaces under equal mixed mode ratios. In both material systems, the surface morphology is strongly dependent upon the direction of the applied Mode II shear load. Direction of hackle tilt and type of fiber failure (tensile or compressive, facing left or right) indicate the direction of the applied shear load. No indication could be seen, except in the Mode I graphite/epoxy, to indicate the direction of crack propagation.

## REFERENCES


1. Wang, A. S. D, and Crossman, F. W., "Initiation and Growth of Transverse Cracks and Edge Delamination in Composite Laminates. Part I. An Energy Method", Journal of Composite Materials Supplement, Vol. 14, 1980.
2. Crossman, F. W., Warren, W. J., Wang, A. S. D, and Law, G. E., Jr., "Initiation and Growth of Transverse Cracks and Edge Delamination in Composite Laminates. Part 2. Experimental Correlation", Journal of Composite Materials Supplement, Vol. 14, 1980.
3. Whitney, J. M., Browning, C. E., and Hoogsteden, W., "A Double Cantilever Beam Test for Characterizing Mode I Delamination of Composite Materials", Journal of Reinforced Plastics and Composites, October 1982.
4. Whitney, J. M., Materials Laboratory, Air Force Wright Aeronautical Laboratories. Private communication.
5. Lakshminarayana, H. V., "A Symmetric Rail Shear Test for Mode II Fracture Toughness (GIIc) of Composite Materials--Finite Element Analysis", to be published.
6. Whitney, J. W., Daniel, I. M., and Pipes, R. B., "Experimental Mechanics of Fiber Reinforced Composite Materials", Society for Experimental Stress Analysis Monograph No. 4, Brookfield Center, Conn (1982).
7. Purslow, D., "Some Fundamental Aspects of Composites Fractography", Composites, Vol. 12, No. 4, October 1981.
8. Bradley, W. L., and Cohen, R. N., "Delamination and Transverse Fracture in Graphite/Epoxy Materials", Proceedings of the Fourth

International Conference on Mechanical Behaviour of Materials, Stockholm (1983).

9. Davidovitz, M., Mittelman, A., Roman, I., and Marom, G., "Failure Modes and Fracture Mechanisms in Flexure of Kevlar-epoxy Composites", Journal of Materials Science 19, 1984.

10. Sinclair, J. H., and Chamis, C. C., "Mechanical Behavior and Fracture Characteristics of Off-Axis Fiber Composites I--Experimental Investigation", NASA Technical Paper 1081, December 1977.

11. Hahn, H. T., and Johnannesson, T., "A Correlation Between Fracture Energy and Fracture Morphology in Mixed-Mode Fracture of Composites", Proceedings of the Fourth International Conference on the Mechanical Behavior of Materials, Stockholm (1983).

12. Kinloch, A. J., and Young, R. J., "Fracture Behaviour of Polymers", Applied Science Publishers (1983).

END

FILMED

10-85

DTIC